IT'IS FOUNDATION

Foundation for Research on Information Technologies in Society

Prof. Dr. Niels Kuster

Director Foundation IT'IS
Professor of Swiss Federal Institute of Technology – ETHZ
Phone +41 1 245 9690 · kuster@itis.ethz.ch

Final Report

Assessment of ELF Exposure from GSM Handsets and Development of an Optimized RF/ELF Exposure Setup for Studies of Human Volunteers

BAG Reg. No. 2.23.02.-18/02.001778

Markus Tuor, Sven Ebert, Jürgen Schuderer, Niels Kuster

Zürich, January 2005

Executive Summary

Mobile communication has increased dramatically over the past decade. The GSM Association predicts about 1.5 billion users of the global digital mobile system by mid 2006. The growing concern of the public HAS led to research projects to investigate possible adverse health effects posed by mobile communication. Although the major focus is on RF radiation, some scientists are concerned about the possible impact of combined exposure to RF and ELF fields.

Magnetic ELF components are mainly generated by supply currents in the phone. The device with the largest power consumption is the front-end amplifier. Consequently, the corresponding ELF magnetic field has a spectrum similar to the pulse structure of RF signals.
The objectives of this study is:

- Development of measurement equipment and protocols to accurately assess the ELF fields from mobile phones.

- Assessment of the ELF exposure from five representative GSM mobile phones.

- Determination of the SAR distribution as well as the spatial peak SAR averaged over 1 g and 10 g.

- Development of a setup enabling the exposure of human volunteers with combined RF/ELF fields under worst-case conditions.

The deliverables of these objectives are reported in this document. Various approaches have been studied; a measurement setup based on two magnetic field sensors, a Coil probe (ELT-400, NARDA, USA) and a Hall sensor (Gaussmeter 7030, F.W. Bell, USA), mounted on a near-field scanning system (DASY4 , SPEAG, Switzerland) has been developed. The B-field sensors and the system have been thoroughly characterized and validated.

In part I of this report the ELF exposure ($\leq$400kHz) of five different GSM phones (Motorola Timeport, Nokia 3310, Sony Ericsson T68, Sony Ericsson T610 and Siemens A50) are examined. The results of the measurements show frequency components as expected by analyzing the GSM signal at 216.7 Hz and 8.3 Hz as well as higher harmonics. When the magnetic fields are extrapolated from the measurement distance at 5 mm to the phones surface, they reach values between 35 μT and 75 μT on the back and between 8 μT and 20 μT on the front side of the mobile phone. The spatial peak SAR and the peak B-field show no correlation; the spatial peak SAR values of the phones range between 0.6 to 1.5 mW/g for 1 g and 0.4 to 1.0 mW/g for 10 g.

Based on the measurements, a worst-case signal is proposed which includes the maximum values for the pulse height, pulse slopes and pulse half width of the measured waveform shapes. This worst-case signal can be used in biomedical laboratory studies investigating the possible effects of ELF or combined RF/ELF fields from mobile phones.

In part II of this report an ELF add-on to an RF exposure setup is presented, which enables the exposure of human volunteers with the proposed ELF worst-case signal in addition to the RF signal.

Keywords

Contents

Part I

ELF Magnetic Field Assessment of Five GSM Phones

1 Introduction

The research currently being conducted to investigate possible adverse health effects posed by radiofrequency (RF) electromagnetic fields (EMF) is substantial. Although the major focus is on RF radiation, some scientists are concerned about the possible impact of combined exposure to RF and extremely low frequency (ELF) fields, especially since mobile phones not only expose the user to RF EMF but also to ELF EMF. Hence, health risk experiments with a combined exposure signal of RF and ELF would best represent the worst-case exposure from a mobile phone.

Digital GSM telephones transmit in the 900 MHz band (890-915 MHz) with a maximum power level of 2 W (peak value) and use the time sharing access scheme TDMA. Within each GSM channel (bandwidth in voice mode 200 kHz) up to eight ongoing calls can be transmitted simultaneously. Thus, GSM phones operate in one of the eight time slots, i.e., sending the information to the base station in 0.577 ms bursts with 217 bursts per second. The multi-frame structure and the advanced power saving features Discontinous Transmission Mode (DTX) of the digital GSM signal result in further occuring frequency components of 8Hz and 2Hz respectivly. The RF spectral power content has been widely examined [Ped97] [PA99] as well as the exposure to RF fields in the human head caused by hand-held mobile phones [KKS97].

The pulsed transmission mode causes pulsed currents in the phone. So the ELF fields are caused by high supply currents inside the phone. The circuit with the highest power consumption is the front-end amplifier which is only active during transmission, i.e., the resulting ELF EMF signal has lower frequency components similar to the demodulated RF signal.

The assessment of these ELF fields requires advanced features of the measurement probe: to determine the frequency components and the pulse form of the ELF magnetic pulses the field probe needs to measure frequencies > 20 kHz for a precise determination of the rise and fall time of the pulse. To measure peak values a local resolution of < 10 mm is necessary, as well as the ability to measure as close to the surface as possible. The average field strength decreases rapidly with distance form the phone surface so that the magnetic field probe needs to be sensitive enough to measure low fields ($\ll 1\,\mu$T).

[JPS04] [LM97] [PA99] [HJC98] examined the ELF magnetic fields from a mobile phone. However, none of them give a complete picture of the ELF EMF exposure including spectral power content, magnetic field strength and magnetic field distribution. Some did not measure the magnetic fields, just the battery currents [JPS04]; others use measurement devices capable of only a few hundred Hertz so that higher harmonics are not sufficiently considered for the actual spectral power content (e.g. [LM97]). The presented studies general show no spatial resolution. None of the studies presented the magnetic field distribution, only peak values (e.g. [PA99]) and waveforms [JPS04].

This study examines for the first time the spectral power content, magnetic field strength, magnetic field distribution and waveform of five GSM mobile phones: Sony Ericsson T610, Siemens A50, Motorola TP, Sony Ericsson T68, and Nokia 3310. Additionally, the SAR distribution with its 10g and 1g spatial peak SAR were measured. From the results a worst-case signal with respect to maximum B-field and maximal frequency components at the surface of

the mobile phone is defined. Further, a suitable setup enabling the exposure of the head of test persons with a combined RF and ELF signal is presented, using the developed worst-case signal. This setup can be used for combined ELF/RF human exposure studies.

2   Material and Methods

2.1   Mobile Phones

The ELF magnetic fields of five mobile phones operating at GSM 900 MHz were determined. To ensure maximum output power (2W, nonDTX), the emission mode was set and controlled by a digital radio tester (Rohde&Schwartz, CTS 55, Germany). The following phones were examined:

- Motorola Timeport

- Siemens A50

- Nokia 3310

- Sony Ericsson T68

- Sony Ericsson T610

Figure 1: Tested phones: Motorola TP, Siemens A50, Nokia 3310, SonyEricsson T68, SonyEricsson T610.

2.2   B-Field Probes

To determine the ELF magnetic fields with spectral power content, magnetic field strength and field distribution as well as the waveform, two different B-field probes were used: Coil probe (ELT-400, NARDA, USA) and Hall meter (Gaussmeter 7030, F.W.Bell, USA). Only this combination enabled a spatial resolution of < 10 mm together with a fast time domain measurement of the field. The waveform was determined with the up to 400 kHz fast 3-axis coil probe and the field distribution with the small dimensioned hall meter (spatial resolution < 5 mm). Both magnetic field sensors were shielded with a metal netting grounded through the device to achieve immunity to the emitted RF of the phone.
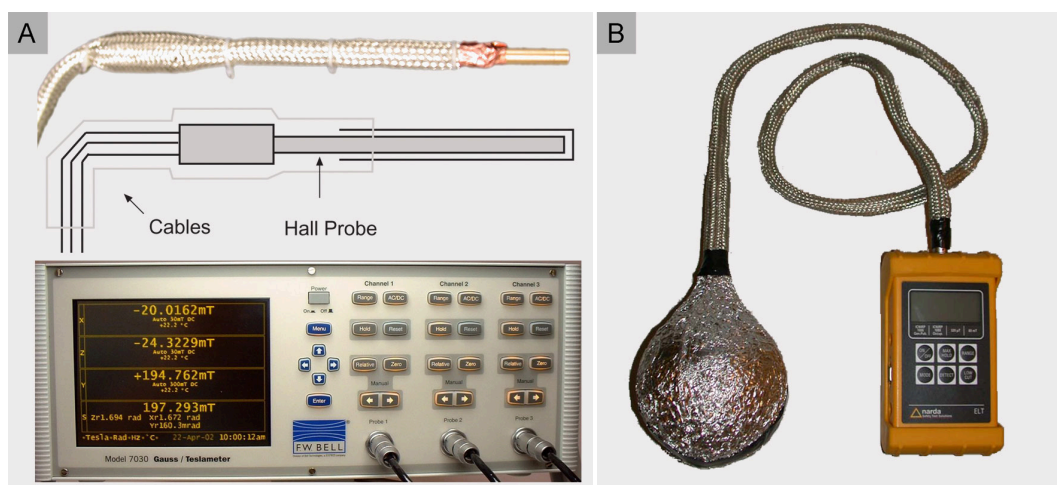
Figure 2: (A) Hall sensor (Gaussmeter 7030, F.W.Bell, USA) and (B) Coil probe (ELT-400, NARDA, USA)

Coil probe

A 3-axis coil probe (ELT-400, NARDA, USA) was used to measure the waveform of the B-field exposure in the time domain (Figure 2). The advantages of the probe include its frequency range of up to 400 kHz and sensitivity to resolve B-fields between 80 nT and 80 mT. The noise level of 80 nT can be reduced down to 10 nT by applying time averaging of 100 ms. The frequency response is shown in Figure 3 (determined by means of a long wire setup). The disadvantage is the large coil diameter of 112 mm, which disables measurements close to the phone surface and provides limited local field information. For RF immunity the probe and cables were shielded with aluminum foil and metal netting (see Figure 2) (RF interference is reduced to less than 70 nT when exposing the probe to a 900 MHz, 16 W power pulse from a dipole antenna in close proximity to the shielded sensor).

Hall meter

A 3-axis Hall meter (Gaussmeter 7030, F.W. Bell, USA) with a standard 3-axis probe (type ZOA73-3208-05-T, F.W. Bell, USA) was used to measure the spatial B-field distribution (Figure 2). The advantage of the Hall sensor is its high local resolution due to the small probe dimensions. The sensors are arranged orthogonally within a $4.8 \times 4.8 \times 5.8 \, \text{mm}^3$ cube with a distance between the tip of the probe and the average sensor location of just 5 mm. The exact positioning of the sensors in the probe was checked using B-field measurements with a known field distribution in a long wire setup. The disadvantages include the low frequency range of the Hall sensor from DC to 400 Hz and a relatively high broadband noise level in the time domain of $1 \, \mu\text{T}$. However, when concentrating the measurements to the 217 Hz component of the B-field signal, fields down to 60 nT are detectable by applying a FFT (Fast Fourier Transformation) to a 5 s sample with a 4 kHz sampling rate. The effective frequency response is shown in Figure 3 (measured using a Helmholtz coil setup). RF interference is minimized by shielding (Figure 2): a thin metal tube covers the front part of the sensor; the sensor's head and wires are enclosed in metal netting. No RF interference was detected when applying a 16 W power pulse via a dipole antenna in close proximity to the probe.
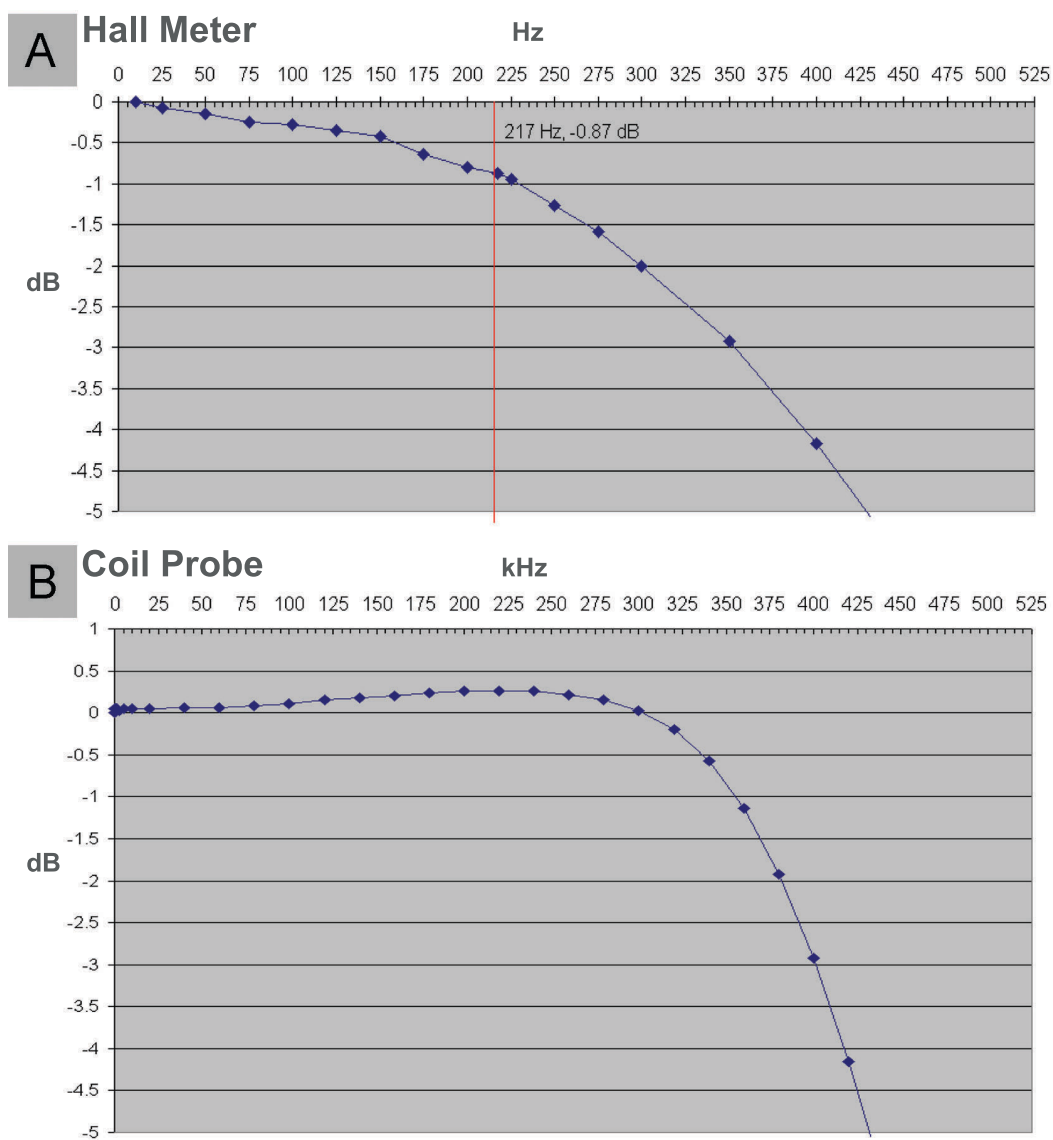
Figure 3: B-field frequency response of the Hall meter and the Coil probe.

2.3 Measurement Procedure

The magnetic field probes were mounted on the industrial robot (RX90L, Staeubli SA, France) of a computer controlled measurement system (DASY4, SPEAG AG, Switzerland) which enables precise positioning of the probes of better than 0.001 mm (see also Figure 4). The magnetic field values from the sensors were acquired using a data acquisition interface (PCI-MIO-16E-1 with Labview 7.0, National Instruments, USA). For data processing Matlab 7 (Mathworks Inc, USA) including Signal Processing Toolbox 6.2.1 and the Curve Fitting Toolbox R14 was used.
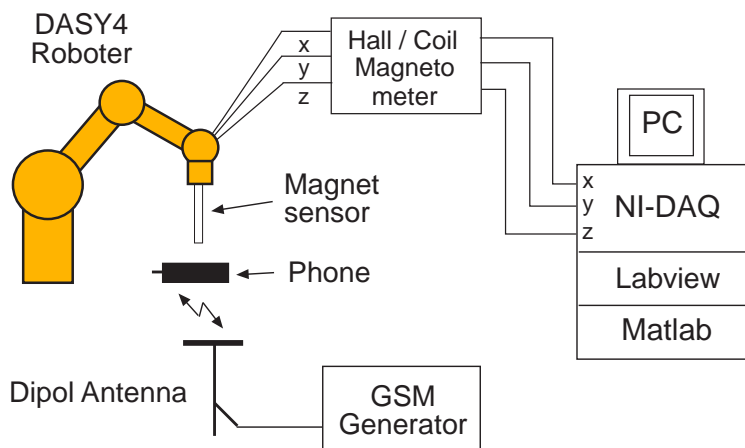

Figure 4: Measurement system consisting of a magnetic field probe mounted on a DASY4 robot and computer controlled field data processing unit.

All five mobile phones were measured using the same procedure:

1. Scanning of the surface B-field distribution on the front and back sides of the mobile phone with the Hall meter detecting the 217 Hz component in a 10 mm grid with the probe touching the phone case. For each data point, an integration time of 5 s at 4 kHz sampling rate was evaluated with the FFT function in the signal processing toolbox of Matlab.

2. Measurement of the B-field decay perpendicular to the surface of the phone with the Hall meter. The measurements were carried out in 1 mm steps in the field maximum as determined by the surface scan.

3. Measurement of the B-field waveform with the coil probe (1.6 MHz sampling rate) at the position where maximal signal to noise ratio was detected. The waveform was averaged in samples of 100 ms (corresponds to ~20 pulses) to reduce the noise level. The full spectrum of the waveform is determined using the FFT of a 10 s sample measured with a sampling rate of 16 kHz.

4. Detection of the maximum DC field on the front and back sides of the phone with the Hall sensor using surface and decay scans. To suppress the DC background level during the measurements (e.g., from the geostatic magnetic field) the Hall sensor output was set to zero when the phone was not yet in place. Then the maximal DC level at the surface of the phone was determined. At the location of the field maximum, the field decay was determined with a z-scan (step size 1 mm).

5. Determination of the SAR distribution of the phones including the corresponding 10 g and 1 g peak spatial peak SAR values in accordance with IEEE P1528/D1.2 using the DASY 4 near-field scanning system (DASY4, SPEAG AG, Switzerland) [IEE03].

2.4 Evaluation Procedure

In order to assess the magnetic field strength, magnetic field distribution, spectral content and waveform of the five GSM mobile phones, the results of the two magnetometers were combined and further evaluated. A worst-case signal was defined based on the resulting maximum values of the five phones.

Magnetic Field Strength on the Phones Surface

For the determination of the magnetic field on the phone surface, the Hall sensor measurements need to be extrapolated by 5 mm (according to the assembly of the probe, the Hall sensors are located on average 5 mm from the phone's surface).

To extrapolate the B-field from the measurement location to the phone surface, an appropriate model of the B-field source which complies with the measured distribution and decay characteristics of the phone was determined: a circular loop model.

The typical B-field distribution of a mobile phone is shown in Figure 5(a). The field distribution shows a strong B-field component perpendicular to the surface in the z-direction. This behavior can be simulated by a circular current-carrying loop parallel to the phone's surface as shown in Figure 5(b) in which the model parameters (1) loop diameter, (2) loop distance from surface and (3) current on the loop are determined through fitting the measured B-field decay curves (see Figure 5).

According to [Jac82] the B-field of a circular loop in z-direction complies with:

$$B_z = \mu_0 I \frac{R^2}{2(R^2 + (r+d)^2)^{3/2}} \tag{1}$$

where B_z is the flux density in the axial direction, radian R of the loop, current I and distance $r + d$ to the loop center. The distance depends on the measured distance to the phone surface r and on the unknown position inside the phone d. The coefficients R, I and d are estimated using least squares fitting from the curve fitting toolbox of Matlab. An example for a fitted curve and the corresponding parameters are shown in Figure 5.

Amplitude Matching of the Waveform

The Hall sensor measured only the 217 Hz component of the B-field. The measured waveform with the Coil probe contains the full spectral information and therefore the ratio between the 217 Hz component to the pulse height of the complete signal. By matching the 217 Hz component of the waveform signal to the extended Hall probe measurement strength, the full spectral power content of the signal at the phone's surface is determined. The B-field spectrum is then the Coil spectrum times the ratio between the 217 Hz component of the extrapolated Hall measurements and the 217 Hz component of the Coil spectrum.

Worst-Case ELF Signal

A worst-case B-field strength has been evaluated based on the extrapolated values for the phone surface, analyzing the B-field pulse for: (1) pulse height, (2) maximum time derivative of the pulse flanks: dB/dt, (3) pulse half width (full width at half maximum), (4) half rise time.
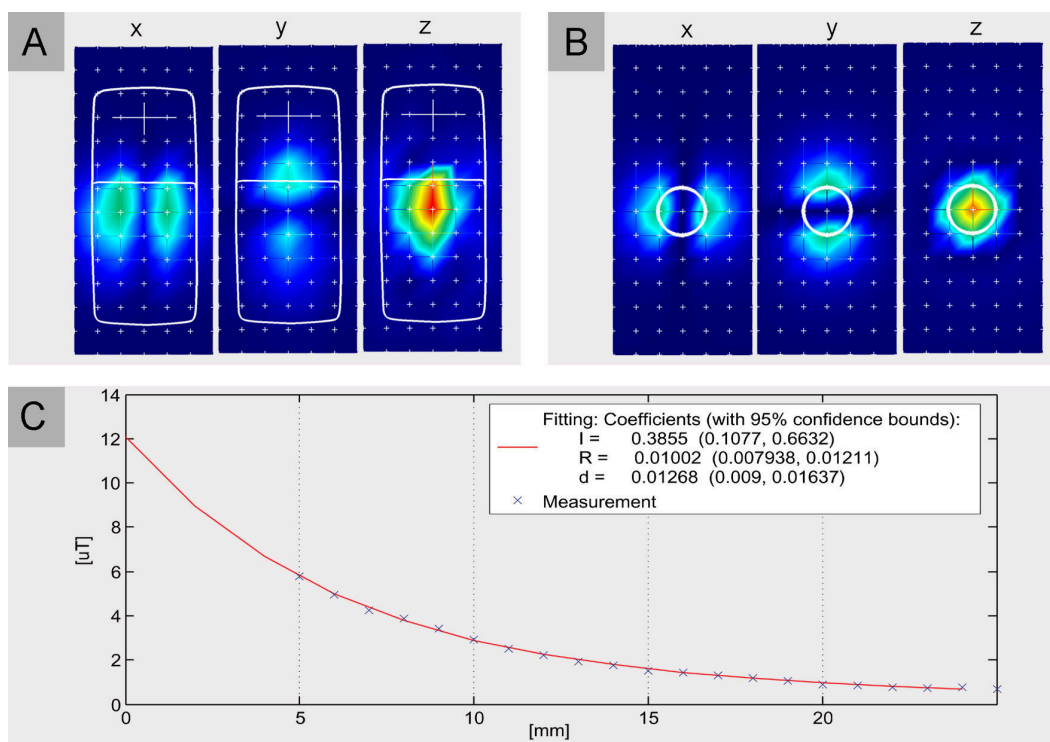
Figure 5: From the same phone (A) the measured B-field distribution in X, Y, Z, (B) the circular loop model B-field distribution and (C) the B-field decay measurement with corresponding fitting curve.

It must be noted that this extrapolation is based on a simplified model and has a considerable uncertainty. When applying the extrapolation model to varying datasets with respect to positioning uncertainty ($\pm$ 0.5 mm) and B-field uncertainty ($\pm$ 60 nT), a standard deviation from the specified values of $15 - 30\%$ was derived, depending on the specific phone model.

3   Results

The measurement results are summarized in two parts:

1. Figures 6 - 10 provide for all five mobile phones:

    (a) B-field distribution on front and back sides. The two distribution pictures show the 217 Hz component of the sum vector of all three axes ($B_s = \sqrt{B_x^2 + B_y^2 + B_z^2}$). The magnitude figured is the result of the surface scan with an average distance of 5 mm between the phone's surface and the sensor position. The position of the phone (white contour) as well as the battery (yellow contour) is sketched in the Figures.

    (b) B-field pulse in the time domain. Waveform measured with the coil probe and pulse height extrapolated to the maximal B-field point on the phone surface.

    (c) B-field spectrum in relation to the ICNIRP reference levels. The spectrum of the B-field pulse at the maximum B-field point. The ICNIRP levels according to [ABB$^+$98].

2. A detailed analysis of all measured and evaluated parameters is given in Table 1. The Table shows B-field parameters of the front and back sides as well as general parameters for each phone, such as waveform aspects, DC fields and SAR values.

    - Front/back side: The first Table section shows values determined individually on both phone sides:
      - Pulse height according to the maximal measured B-field strength during the surface scan (5 mm distance to surface) and pulse height according to the extrapolated maximal B-field strength on the phone surface (0 mm distance to surface).
      - Maximal slope of the up/down flank according to the maximal pulse extrapolated to the phone surface (0 mm distance to surface).
      - Fit coefficients used for the B-field extrapolation model in order to determine the maximal B-field strength directly on the surface (0 mm distance to surface). The coefficients represent current, radian and position of the wire loop model.
    - Pulse Form: Pulse half width (full pulse width at half rise of the pulse) and half rise time (the rise time until half of the pulse height is reached).
    - DC B-field: Strongest measured DC field (5 mm to surface) and maximal extrapolated DC field (0 mm to surface).
    - Spatial peak SAR: The 1g and 10g peak spatial average specific absorption rate (SAR).
    - Ratio to ICNIRP Limit: Represents the violation of the ICNIRP reference levels for 217 Hz and harmonic components.
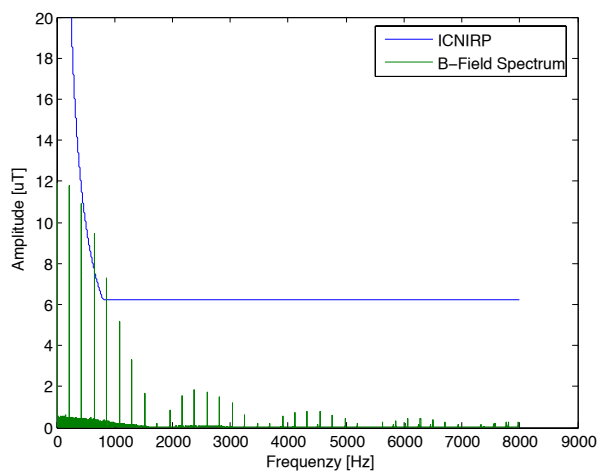
Figure 6: Motorola Timeport
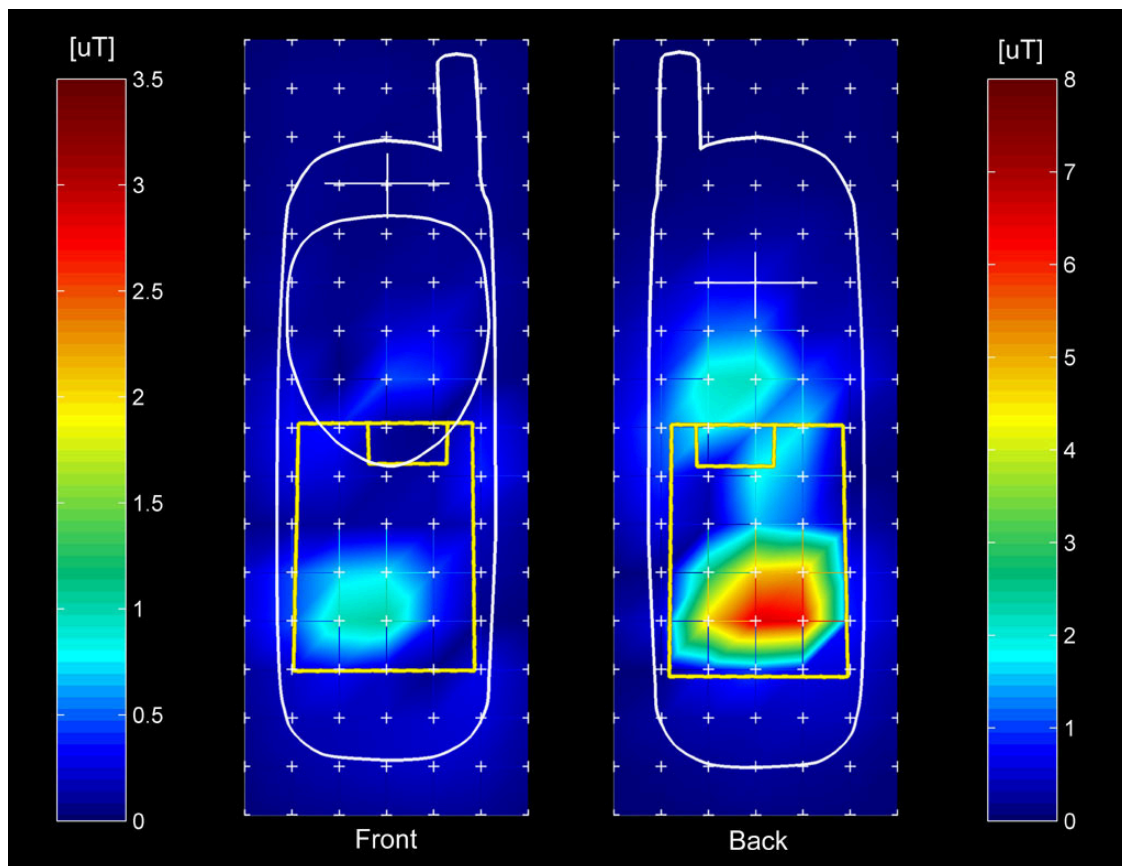
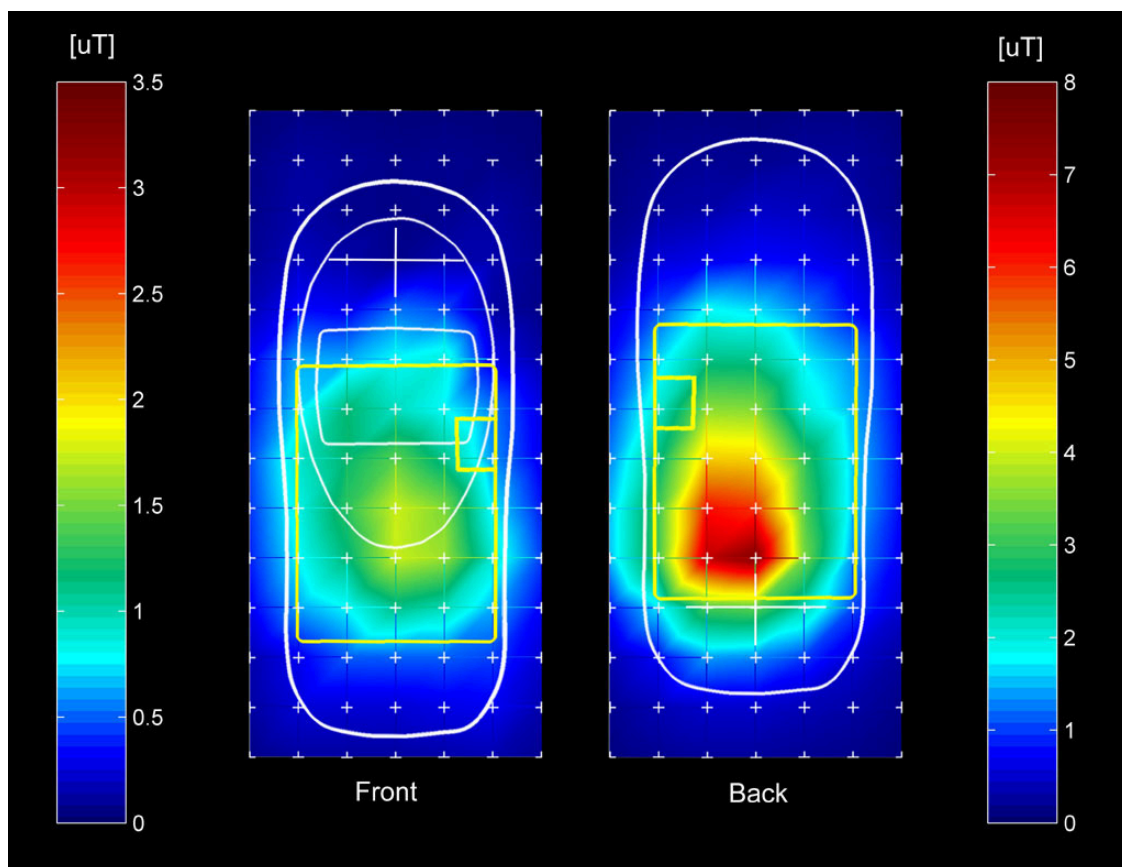(a) Surface scan, front and back sides, yellow drawing represents battery.
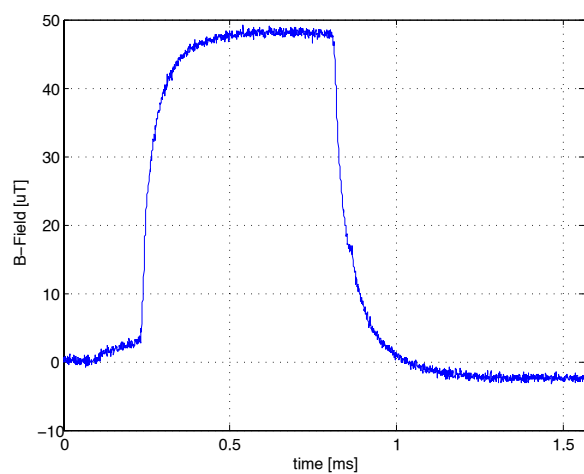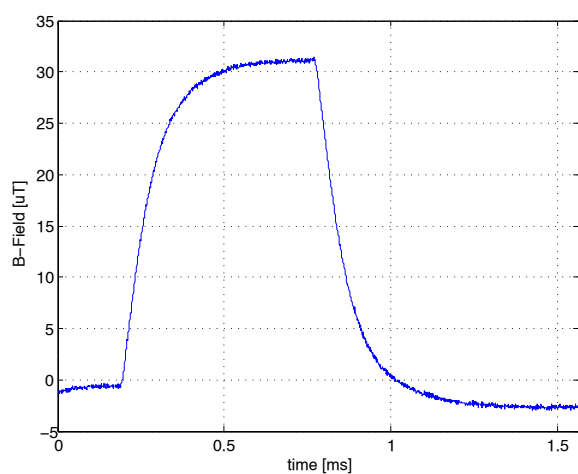

(b) Waveform, worst case
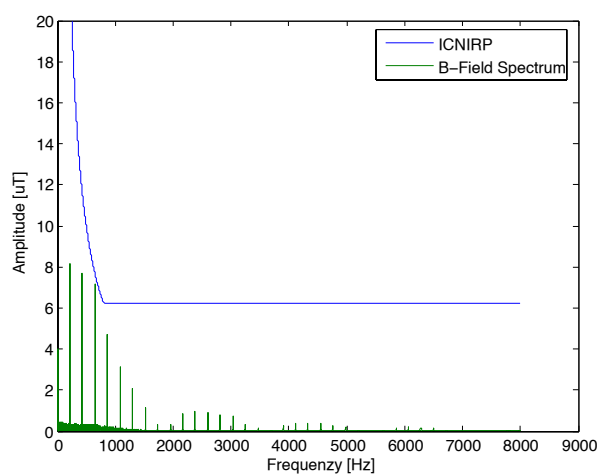

(c) Spectrum, worst case

Figure 7: Siemens A50

(a) Surface scan, front and back sides, yellow contour represents battery.
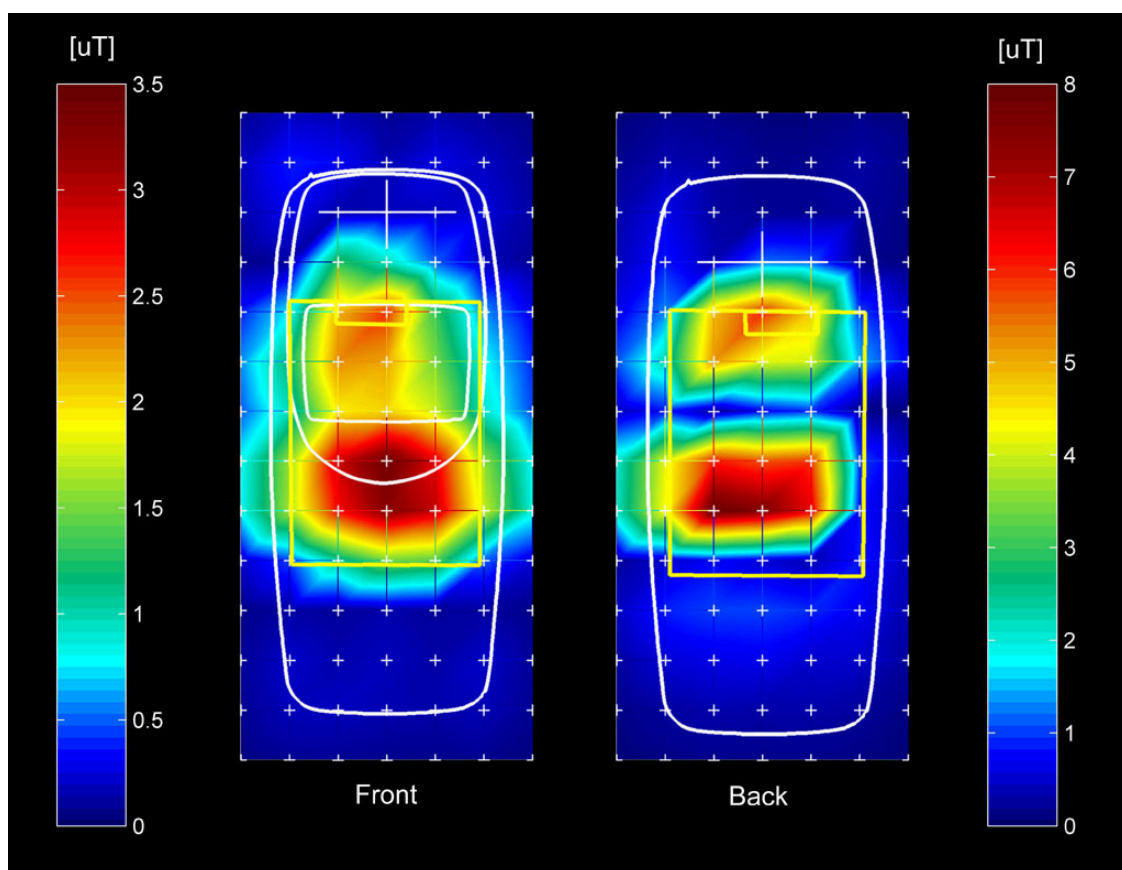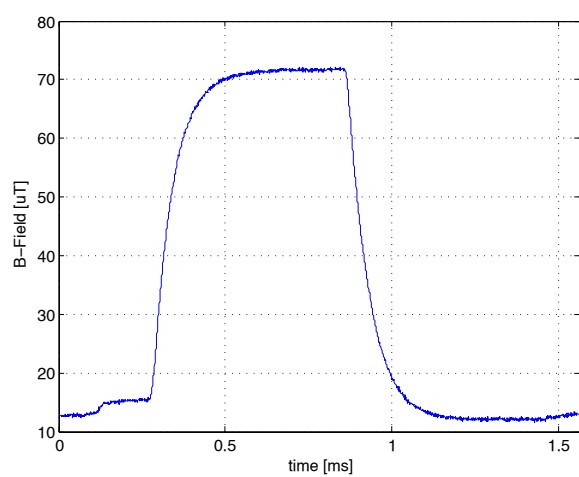

(b) Waveform, worst case
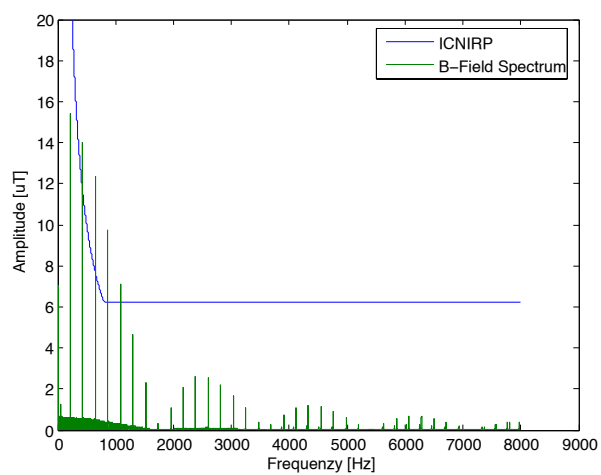

(c) Spectrum, worst case

Figure 8: Nokia 3310

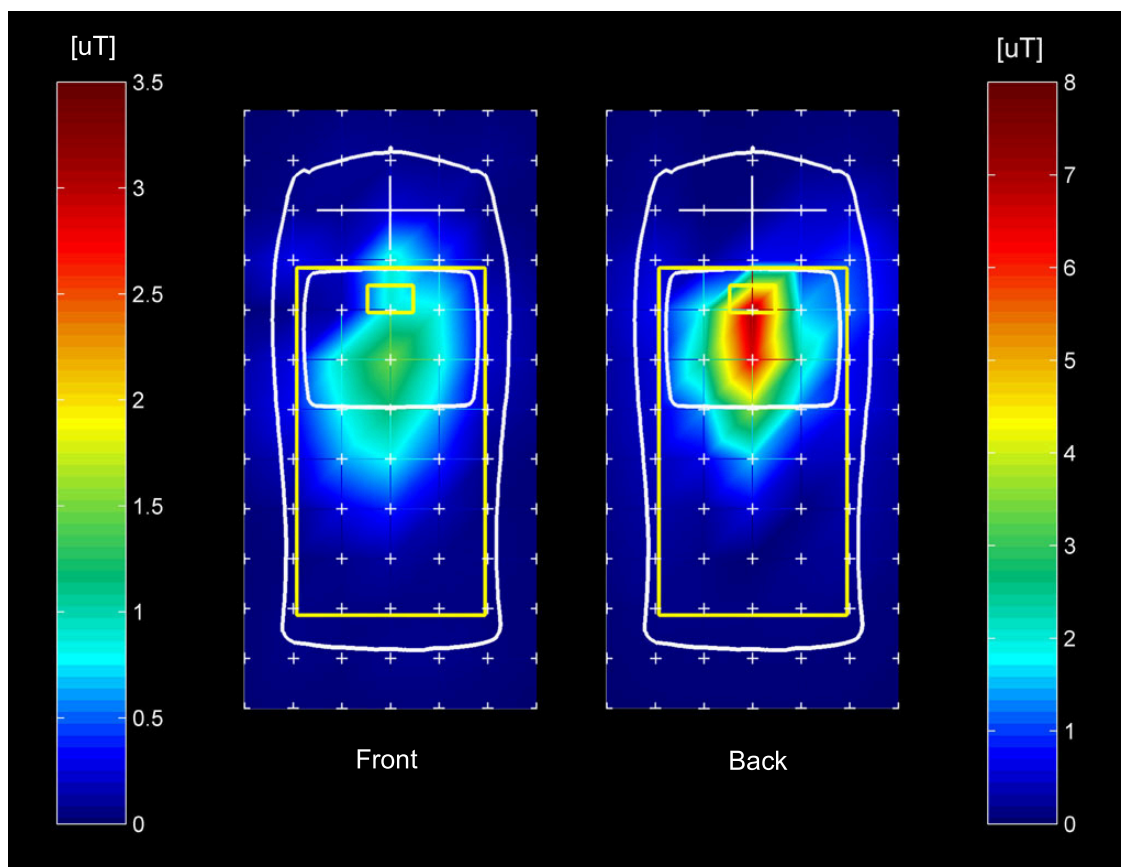(a) Surface scan, front and back sides, yellow contour represents battery.

(b) Waveform, worst case

(c) Spectrum, worst case

Figure 9: Sony Ericsson T68

(a) Surface scan, front and back sides, yellow contour represents battery.

(b) Waveform, worst case

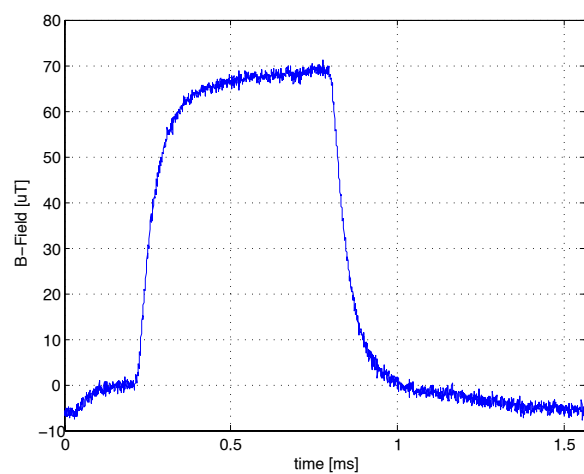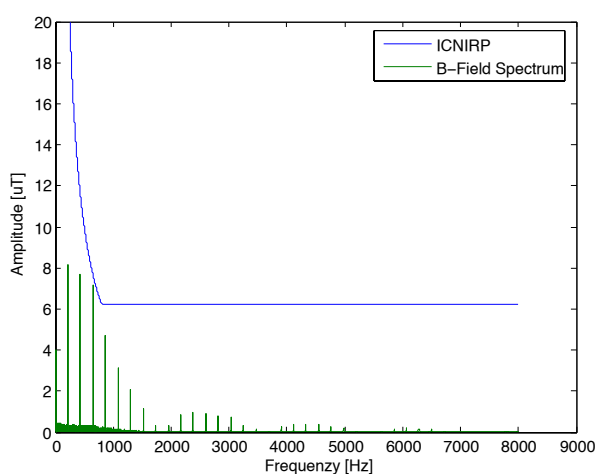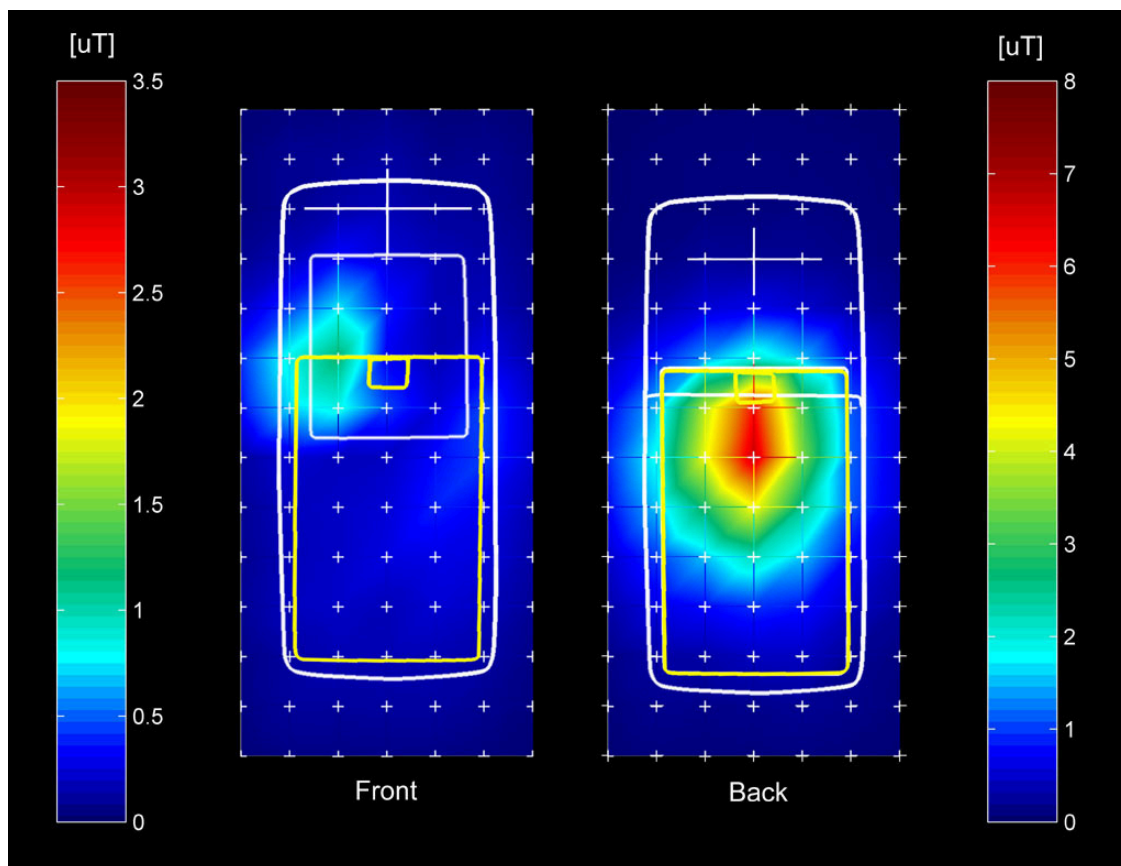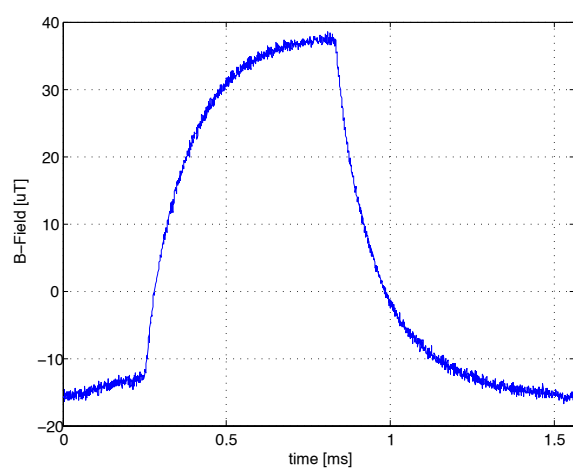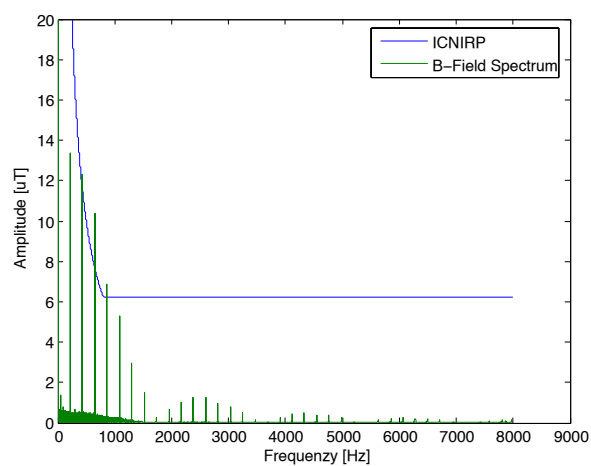(c) Spectrum, worst case

Figure 10: Sony Ericsson T610

(a) Surface scan, front and back sides, yellow contour represents battery.

(b) Waveform, worst case

(c) Spectrum, worst case

Table 1: **Mobile phone field measurement results**

	Motorola Timeport	Siemens A50	Nokia 3310	SonyEricsson T68	SonyEricsson T610
Front side					
Pulse height, 5 mm[a]	4.70 μT	7.52 μT	14.63 μT	6.09 μT	4.94 μT
Pulse height, extp.[b]	8.3 μT	12.4 μT	19.3 μT	8.3 μT	11.7 μT
Max dB/dt, extp.[b], up slope	0.23 T/s	0.10 T/s	0.26 T/s	0.13 T/s	0.10 T/s
Max dB/dt, extp.[b], down slope	-0.21 T/s	-0.11 T/s	-0.28 T/s	-0.13 T/s	-0.10 T/s
Fit coefficients for extrapolation[c]					
I	0.23 A	0.22 A	0.51 A	0.069 A	3.8 A
R	0.008 m	0.014 m	0.021 m	0.018 m	0.002 m
d	0.021 m	0.022 m	0.030 m	0.013 m	0.019 m
Back side					
Pulse height, 5 mm[a]	29.46 μT	31.89 μT	33.68 μT	29.50 μT	28.07 μT
Pulse height, extp.[b]	52.8 μT	35.1 μT	66.1 μT	74.8 μT	56.3 μT
Max dB/dt, extp.[b], up slope	1.43 T/s	0.29 T/s	0.88 T/s	1.14 T/s	0.50 T/s
Max dB/dt, extp.[b], down slope	-1.33 T/s	-0.30 T/s	-0.97 T/s	-1.14 T/s	-0.50 T/s
Fit coefficients for extrapolation[c]					
I	0.29 A	0.21 A	1.57 A	0.85 A	0.38 A
R	0.013 m	0.016 m	0.009 m	0.007 m	0.010 m
d	0.011 m	0.009 m	0.020 m	0.014 m	0.013 m
Pulse form					
Half width	0.59 ms	0.58 ms	0.58 ms	0.58 ms	0.59 ms
Half rise time	24 ns	68 ns	47 ns	39 ns	88 ns
DC B-field					
at 5 mm[a] distance	5.3 mT	1.6 mT	2.7 mT	4.1 mT	1.5 mT
extrapolated[b]	20.2 mT	3.4 mT	8.6 mT	13.1 mT	3.9 mT
Spatial peak SAR					
SAR (1g)	1.21 mW/g	1.54 mW/g	1.49 mW/g	0.616 mW/g	1.16 mW/g
SAR (10g)	0.826 mW/g	1.01 mW/g	1.02 mW/g	0.438 mW/g	0.707 mW/g
Ratio to ICNIRP limit					
217 Hz	≤ 1	≤ 1	≤ 1	≤ 1	≤ 1
1st harmonic: 433 Hz	≤ 1	≤ 1	1.2	1.5	1.1
2nd harmonic: 650 Hz	1.2	≤ 1	1.6	2.0	1.3
3rd harmonic: 867 Hz	1.2	≤ 1	1.6	1.7	1.1
4th harmonic: 1083 Hz	≤ 1	≤ 1	1.1	1.4	≤ 1

[a] Signal 5mm from surface (probe touching surface) at maximal B-field point (217 Hz or DC)

[b] Extrapolated signal on surface at maximal B-field point

[c] Fit coefficients for extrapolation: current I, radian R and distance d

4   Discussion and Generic Test Signal

The five tested phones show considerably different B-field waveforms and amplitudes. Whereas the pulse width is similar for all phones and corresponds to the GSM RF pulse width of 0.58 ms, the pulse shapes show individual characteristics with respect to their half rise times, which are vary between 24 and 88 ns. All phones show the maximum B-field on the back side with extrapolated pulse heights between 35 and 75 μT. At this location, four out of the five tested phones exceed of the ICNIRP reference levels by several harmonics of 217 Hz. The maximum violation by a factor of two was detected at 650 Hz. The B-field on the front side of the phones tested is by a factor of 2 - 6 times smaller and varies between 8 and 20 μT. The B-field distribution shows a localized field maximum near the battery, whereby the field is dominantly polarized perpendicular to the phone surface. Hence, the current distribution on the phone can be approached by a horizontal current loop in the battery region. In contrast, the maximum DC fields were detected near the phone loudspeaker and reach levels up to 20 mT (half of the corresponding ICNIRP reference level of 40 mT). The SAR measurements revealed spatial peak SAR values between 0.6 - 1.5 mW/g (1g) and 0.4 - 1.0 mW/g (10g). No correlation between the spatial peak SAR and the peak B-field can be seen.

It is important to note that the ICNIRP basic restrictions for ELF magnetic fields are primary focused on induced current density. Mathematical modeling of the human body and extrapolation were applied to derive the reference levels for the magnetic field strength. Since the current density is a function of the spatial averaged B-field times the cross section of the induced current paths, localized B-fields will lead to considerably fewer induced currents than the anticipated ICNIRP worst-case of a homogeneously distributed B-field across the entire human body. Therefore, the reported B-field violations do not necessarily correspond to violations in current density; for the latter, they are rather expected to lead to less or no violation. However, further investigations are needed to assess the induced currents resulting from ELF mobile phone exposure in detail. Based on the results in Table 1, a worst-case ELF B-field exposure signal is proposed, which can be used in biomedical laboratory studies investigating the possible effects of ELF or combined RF/ELF fields from mobile phones. The selection criteria were:

- Maximized B-field strength

- Maximized spectral power

Based on this criteria we propose the ELF exposure signal of Table 4 to be used in combination with RF.

Table 2: **Worst-case signal parameters**

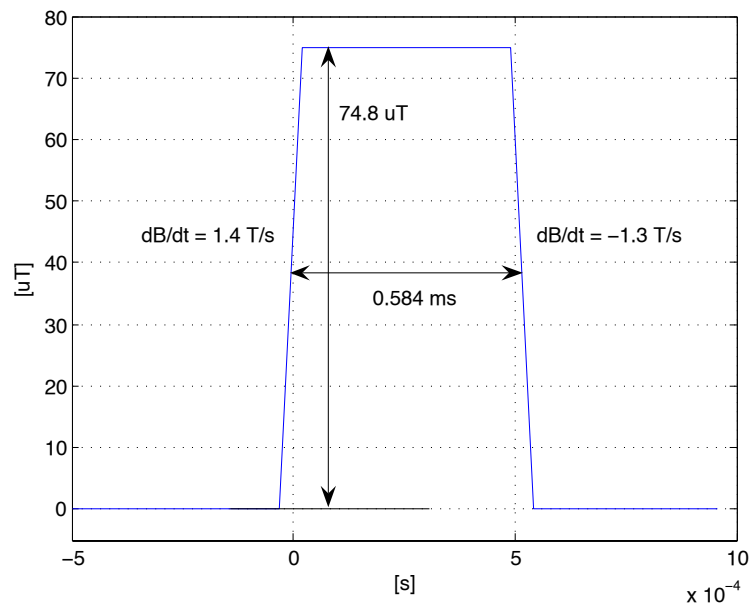|	
Pulse height:	75 μT (max of 5 phones)
Pulse slope up:	1.4 T/s (max of 5 phones)
Pulse slope down:	-1.3 T/s (min of 5 phones)
Pulse half width:	0.584 ms (average of 5 phones)

Figure 11: Generic Worst-Case ELF Test Signal generated from the measurement results of five GSM phones (1) pulse height: 75 μT (max of 5 phones), (2) pulse slope up: 1.4 T/s (max of 5 phones), (3) pulse slope down: -1.3 T/s (min of 5 phones) and (4) pulse half width: 0.584 ms (average of 5 phones).

Part II
Exposure Setup for Combined RF/ELF Human Exposure Study

5 Objectives

Human provocative studies such as [HkK$^+$05] [HSG$^+$03] are usually performed by exposing the test person's head with a worst-case RF signal. To take into account both RF and ELF exposure from mobile phones, existing RF exposure setups need to be extended with an ELF exposure add-on, as presented here. In Part I the worst-case ELF magnetic field signal was defined as a result from the ELF MF measurements of five GSM mobile phones. This proposed ELF exposure add-on exposes the test persons head to the worst-case signal with 95 % homgeneity in head volume.

6 Setup Design: ELF Add-On

The proposed design for the RF/ELF exposure system is based on an update of the RF exposure system as described in Huber et al., 2003 [HSG$^+$03]. A sketch of the configuration is given in Figure 12.
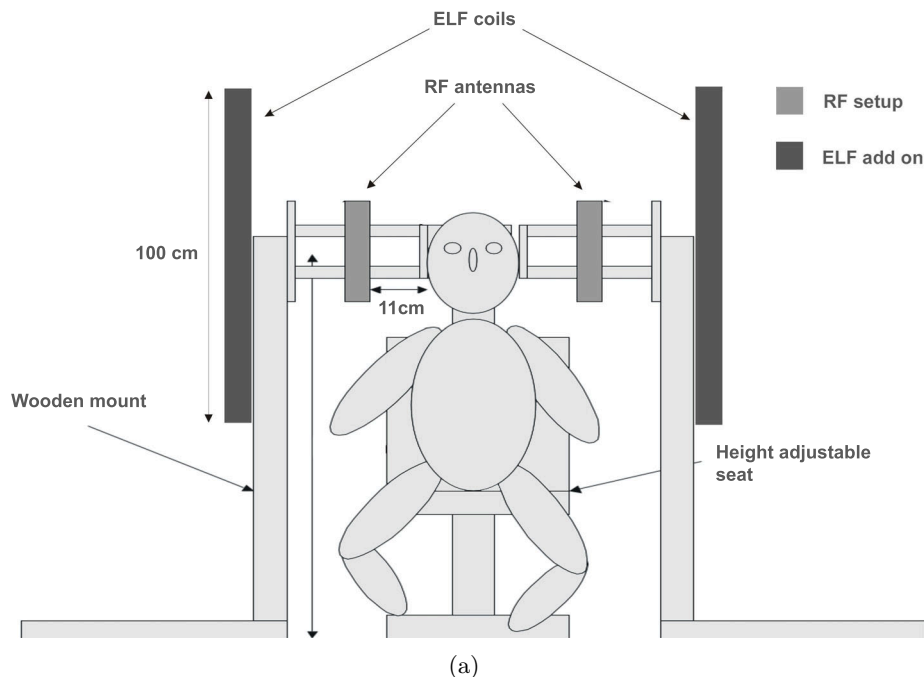

(a)

Figure 12: Front view of a combined ELF and RF exposure setup. The ELF add-on is shown in dark gray.

Two square coils with a side length of 1 m are arranged in parallel at a distance of 0.88 m. The coils are mounted exteriorly on two wooden racks which are placed on both sides of the test person. Hence, the head of the test person and the RF setup (which is based on two

patch antennas) are located between the coils. The coil configuration does not exactly meet the Helmholtz condition (distance between coils = coil radius) but was chosen in order to keep the coil size moderate and still provide a homogeneous B-field distribution across the human head. No interaction between the B-field and the RF setup is present, because the RF setup is based only on non-magnetic materials. The coil wires are shielded by copper foil in order to prevent RF coupling into the ELF current circuit. The coil setup does not interfere with the RF exposure, because the coils are located at a sufficiently far distance and behind the patch antenna back planes. Each coil is based on 10 windings with a 1 mm diameter copper wire resulting in an ohmic resistance of $1.88\,\Omega$. To minimize vibrations, the wires are glued together by epoxy resin.

7 B-Field Strength and Distribution

The B-field exposure from the coil setup was analytically investigated in order to determine the B-field vs. current efficiency and the homogeneity of the resulting B-field distribution. The equations according to [MSK$^+$93, 3.1.1 Magnetic field of rectangular loops of many turns] were used to calculate the vector components of the B-field. The resulting field distribution at pulse maximum is shown in Figure 13 with the head area indicated as a red box.

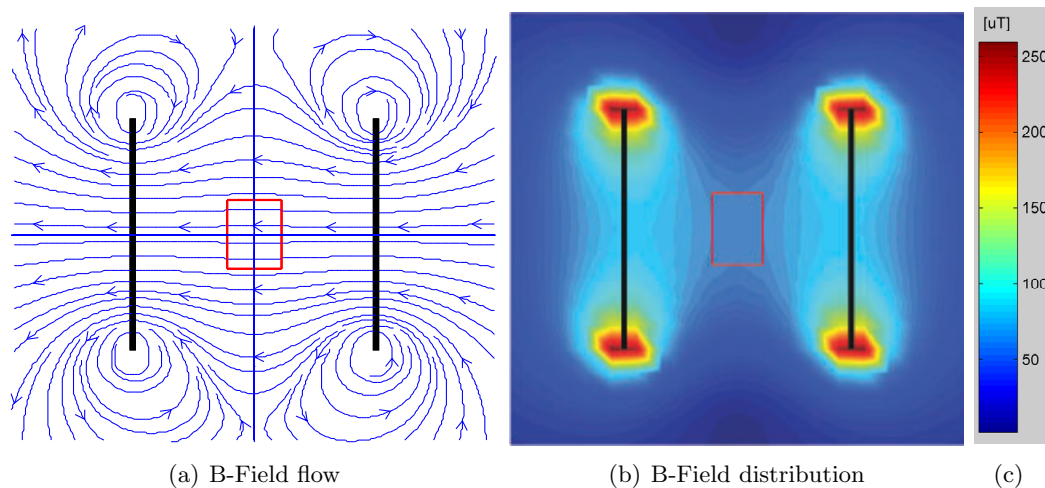(a) B-Field flow   (b) B-Field distribution   (c)

Figure 13: Simulated B-field of rectangular loops. The red box represents the head area.

A homogeneous distribution is present, although the Helmholtz condition is not exactly met. To evaluate the homogeneity in the head area, the average B-field together with minimum, maximum and standard deviation were determined. Hereby, the head area was assumed to be located in the center of the coils, with the dimensions of 15 cm ($\pm 3cm$) x 0.2 m x 0.3 m (width x depth x height). A current of 1 A generates a $10.8\,\mu$T average B-field with a spatial inhomogeneity (standard deviation) of 2.1 % (maximal deviation: 2.8 %, minimal deviation: -4.3 %). The effect of varying head width was further investigated, since it determines the effective coil distance and may represent a source of inter-subject variability. Two worst-cases with a minimum head width of 12 cm and a maximum head width of 18 cm were analyzed, and the resulting B-field efficiency and standard deviation were calculated (Table 3). No significant changes from the reference configuration (deviations < 3.3 %) were derived.

Table 3: **B-field Efficiency and Nonuniformity for Varying Head Width**

	Head width 15 cm	Head width 18 cm	Head width 12 cm
B-field efficiency, B_{avg}/I	10.8 μT/A	10.5 μT/A (-3.3%)[a]	11.1 μT/A(+2.7%)[a]
Spatial B-field inhomogeneity[b]	2.1 %	3.2 %	1.5 %
Maximal deviation[c]	4.0 %	5.1 %	1.8 %

[a] Relative deviation to the reference configuration with head width 15 cm

[b] Standard deviation of B-field in head volume

[c] Maximal B-field deviation in head volume

8 Current Requirements

The current for the coil setup is generated by an arbitrary function generator, combined with a voltage controlled high-current source. In order to produce the proposed worst-case generic test signal, a B-field amplitude of up to 75 μT with pulse slopes of 1.4 T/s / -1.3 T/s (rise/fall) must be achieved. The current amplifier must fulfill the following power requirements in order to generate the B-fields of Table 4.

- Current to produce a 75 μT B-field: I = 6.9 A

- Current flank to produce a 1.4 T/s B-field slope: dI/dt: $1.23 \cdot 10^5$ A/s

- Voltage drop across the coil setup: U = 21 V ($U = L\frac{dI}{dt}$)

The inductance L of the coil setup was determined numerically by calculating the magnetic flux and using the relation $L = 2\frac{d\Phi}{dt}$, where Φ is the flux through one of the coils (2 coils in series). An inductance of 73 nH was found.

9 Summary ELF Add-on Setup

Table 4 summarizes the specifications for the ELF add-on coil setup, including the current requirements for the amplifier. The presented add-on upgrades the existing RF exposure setup for combined ELF/RF studies in the context of mobile phone health risk assessment.

Table 4: **ELF Exposure Setup Specifications**

Side length of square loops	1 m
Distance between loops	0.88 m ($\pm$ 3 cm, head with variation)
Number of windings	10
Coil resistance	R = 1.88 Ohm
Coil inductance	L = 73 nH
B-field efficiency	B^*_{avg}/I = 10.8 μT/A
Spatial B-field inhomogeneity	2.1%
Current requirements for pulse peak	I = 6.9 A
Maximum current flank	$\frac{dI}{dt}$ = $1.23 \cdot 10^5$ A/s
Voltage requirements	U = 21 V

* B_{avg}: Average B-field in head volume

Acknowledgments

References

[ABB+98] A. Ahlbom, U. Bergqvist, J. H. Bernhardt, J. P. Cesarini, L. A. Court, M. Grandolfo, M. Hietanen, A. F. McKinlay, M. H. Repacholi, D. H. Sliney, J. A. J. Stolwijk, M. L. Swicord, L. D. Szabo, M. Taki, T. S. Tenforde, H. P. Jammet, and R. Matthes. Guidelines for limiting exposure to time-varying electric, magnetic, and electromagnetic fields (up to 300 ghz). *Health Physics*, 74(4):494–522, 1998.

[HJC98] B. Heath, S. Jenvey, and I. Cosic. Investigation of analogue and digital mobile phone low frequency radiation spectrum characteristics. In B. Lithgow and I. Cosic, editors, *Proceedings of the 2nd International Conference on Bioelectromagnetism. 15 18 Feb. 1998 Melbourne, Vic., Australia*, pages vii+206. IEEE, New York, NY, USA, 1998.

[HkK+05] L. Hillert, T. kerstedt, N. Kuster, A. Lowden, M. Berg, C. Wiholm, S. Ebert, S. D. Moffat, and B. B. Arnetz. The effects of 900 mhz gsm wireless communication signal on subjective sympton, physiological reactions, alertness, performance and sleep, an experimental provocation study. In *2005 The Bioelectromagnetics Society*, Dublin, Ireland, 2005.

[HSG+03] R. Huber, J. Schuderer, T. Graf, K. Jutz, A. A. Borbely, N. Kuster, and P. Achermann. Radio frequency electromagnetic field exposure in humans: Estimation of sar distribution in the brain, effects on sleep and heart rate. *Bioelectromagnetics*, 24(4):262–276, 2003.

[IEE03] IEEE. Recommended practice for determining the peak spatial-average specific absorption rate (sar) in the human head from wireless communications devices: Measurement techniques. Technical report, IEEE standard 1528 - 2003, 2003.

[Jac82] J. D. Jackson. *Klassische Elektrodynamik*. Walter de Gruyter, Berlin/New York, 1982.

[JPS04] K. Jokela, L. Puranen, and A. P. Sihvonen. Assessment of the magnetic field exposure due to the battery current of digital mobile phones. *Health Physics*, 86(1):56–66, 2004.

[KKS97] N. Kuster, R. Kastle, and T. Schmid. Dosimetric evaluation of handheld mobile communications equipment with known precision. *Ieice Transactions on Communications*, E80B(5):645–652, 1997.

[LM97] T. Linde and K. H. Mild. Measurement of low frequency magnetic fields from digital cellular telephones. *Bioelectromagnetics*, 18(2):184–6, 1997.

[MSK+93] M. Misakian, A. R. Sheppard, D. Krause, M. E. Frazier, and D. L. Miller. Biological, physical, and electrical parameters for in-vitro studies with elf magnetic and electric-fields - a primer. *Bioelectromagnetics*, pages 1–73, 1993.

[PA99] G. F. Pedersen and J. B. Andersen. Rf and elf exposure from cellular phone handsets: Tdma and cdma systems. *Radiation Protection Dosimetry*, 83(1-2):131–8, 1999.

[Ped97] G. F. Pedersen. Amplitude modulated rf fields stemming from a gsm/dcs-1800 phone. *Wireless Networks*, 3(6):489–98, 1997.